Thermal Distribution of Relativistic Particle Beams with Space Charge

Martin Reiser and Nathan Brown
Laboratory for Plasma Research, University of Maryland, College Park, Maryland 20742
(Received 5 April 1993; revised manuscript received 27 August 1993)

The Maxwell-Boltzmann ("thermal") distribution constitutes the natural thermodynamic equilibrium state for a charged particle beam, and knowledge of its properties is therefore of fundamental importance. The Boltzmann relation for the particle density has a nonanalytic form when the space-charge force is included. We use numerical integration to determine the transverse and longitudinal density profiles for a relativistic beam in a linear focusing system at different temperatures $T_\perp$ and $T_\parallel$. The calculated profiles are related to space-charge tune depression, rms width, perveance, and emittance of the beam.

PACS numbers: 41.85.Ew, 29.17.+w, 29.20.−c, 52.25.Wz

Many advanced charged particle beam experiments and applications, such as high-power microwave sources, free electron lasers, linear accelerators for heavy-ion inertial fusion, spallation neutron sources, radioactive waste transmutation, high-energy colliders, and other uses, require very high beam intensity so that the beam dynamics depend strongly on the particle density profile. It is therefore of fundamental interest to know the equilibrium state of the charged particle beam for a given situation. Thermodynamically, this equilibrium state is best described by a Maxwell-Boltzmann ("thermal") distribution with different transverse and longitudinal temperatures ($T_\perp$ and $T_\parallel$) since in practice many beams are not equipartitioned. Many effects lead to coupling between $T_\perp$ and $T_\parallel$ [1]; we deal here with cases where the coupling is small. When space-charge forces are significant the equilibrium density profiles have a nonanalytic form and must be found numerically, which explains why the thermal distribution has received less attention in the literature on beam theory than it deserves. Lawson [2] has published numerical results for the radial density profiles of a continuous nonrelativistic thermal beam in a linear focusing channel. In our work reported here we extend Lawson's results by including the relativistic factor γ^2, correcting an error, and correlating the density profiles with space-charge tune depression, perveance, and emittance of the rms equivalent uniform (K-V) beam. In addition, we determine the line-charge density profiles for a bunched beam with linear longitudinal focusing forces for different longitudinal temperatures and relate the results to the tune depression and other parameters of the rms equivalent parabolic bunch.

The equilibrium distribution f of a group of charged particles in a focusing channel can be found from the Vlasov equation. We assume that the potential can be written as the sum of a transverse potential $\phi_\perp(r)$ and a longitudinal potential $\phi_\parallel(z)$ in cylindrical coordinates, and that the beam and focusing system are uniform, or "smooth." Each of these potentials is the sum of a self-component [$\phi_{\perp s}(r)$ and $\phi_{\parallel s}(z)$] and an external focusing component [$\phi_{\perp e}(r)$ and $\phi_{\parallel e}(z)$].

The Maxwell-Boltzmann distribution has the form $f=f_0\exp(-H/k_BT)$, where H is the single-particle Hamiltonian, k_B is Boltzmann's constant, and T is the temperature. It is a very special case of this class of equilibrium distributions in that it satisfies both the steady-state Vlasov equation as well as the Fokker-Planck equation which includes the effects of collisions (see Ref. [1], Chap. 5.4). Because of the longitudinal cooling by acceleration and other effects, a charged particle beam is generally not in a 3D equilibrium; i.e., the longitudinal temperature $T_\parallel$ differs from the transverse temperature $T_\perp$. We therefore write the distribution in the form

$$f=f_0\exp(-H_\perp/k_BT_\perp)\exp(-H_\parallel/k_BT_\parallel)\,. \tag{1}$$

For a relativistic beam with nonrelativistic transverse and longitudinal velocities in the beam frame where the centroid is at rest, the Hamiltonian for the laboratory frame is given by

$$H_\perp=\gamma_0\frac{m}{2}v_\perp^2+q\phi_\perp,\quad H_\parallel=\gamma_0^3\frac{m}{2}(\Delta v_\parallel)^2+q\phi_\parallel\,, \tag{2}$$

where m is the mass and q the charge of the particles, $v_\perp$ is the transverse velocity, $\Delta v_\parallel=v_\parallel-v_0$ is the relative longitudinal velocity with respect to the mean (centroid) velocity v_0, $\gamma_0=(1-\beta_0^2)^{-1/2}$, $\beta_0=v_0/c$, and c is the speed of light. The "laboratory" temperatures are related to the beam-frame temperature T_0 by $T=T_0/\gamma_0$, and are defined by $\gamma_0 m\overline{v_\perp^2}=2k_BT_\perp$, $\gamma_0^3 m\overline{(\Delta v_\parallel)^2}=k_BT_\parallel$. By integrating the distribution (1) over the velocities one obtains the well-known Boltzmann relation [$\sim\exp(-q\phi/k_BT)$] for the transverse and longitudinal density profiles. We solve for two general cases: (A) the radial profile of an infinitely long beam and (B) the longitudinal profile of a bunched beam.

The radial density profile for case (A) can be obtained by integrating the Poisson equation over the radius r and substituting into the Boltzmann relation, which yields

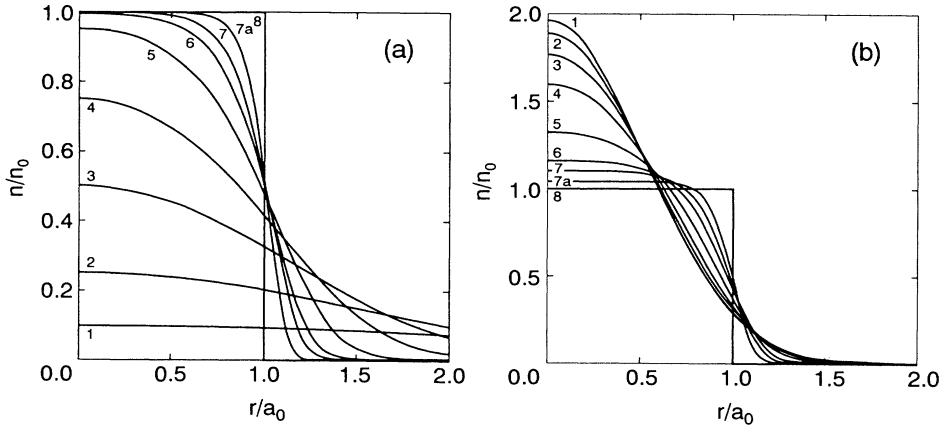

FIG. 1. Particle density of the thermal distribution as a function of radius for different temperatures. In (a) the external focusing force is constant; in (b) the focusing is changed to yield the same rms radius for each curve. The pertinent parameters are listed in Table I.

$$\frac{n(r)}{n(0)} = \exp\left[-\frac{q\phi_{\perp e}(r)}{k_B T_\perp} + \frac{q^2}{\epsilon_0 k_B T_\perp \gamma_0^2} \int_0^r \frac{1}{r'} \int_0^{r'} r'' n(r'') dr'' dr' \right]. \tag{3}$$

The factor γ_0^2 in the denominator of the integral term represents the attraction ($1-\beta_0^2=\gamma_0^{-2}$) due to the magnetic self-forces of the beam. Lawson [2] has solved Eq. (3) numerically for a nonrelativistic beam ($\gamma_0=1$) in a linear focusing channel defined by the potential $\phi_{\perp e}(r) = \frac{1}{2}\gamma_0 mc^2\beta_0^2 k_0^2 r^2$, where k_0 is the focusing wave constant. In Fig. 1(a) we reproduce for ease of comparison Lawson's radial density profiles for eight temperatures with an additional curve (7*a*), and in Fig. 1(b) we have normalized these profiles so that the rms radius remains constant. The profile is exactly uniform at $T_\perp=0$, and at low temperatures, it falls off at the edge in a distance on the order of the Debye length, as shown analytically by O'Neil and Driscoll [3] and by Hofmann and Struckmeier [4]. At high temperature ($T_\perp \to \infty$) or high energy when space-charge forces are negligible, the profile approaches a Gaussian shape, consistent with observations in high-energy accelerators and storage rings [5].

The parameter $\lambda_D(0)/a_0$, the Debye length on axis divided by the radius of the zero-temperature beam, a_0, can be calculated for each of these curves by the relation

$$\frac{\lambda_D(0)}{a_0} = \left[\frac{\epsilon_0 k_B T_\perp \gamma_0^2}{q^2 N_L} \right]^{1/2} \left[\frac{\pi n_0}{n(0)} \right]^{1/2}, \tag{4}$$

where $n_0 = 2\epsilon_0\gamma_0 mc^2\beta_0^2 k_0^2/q$ is the density of the zero-temperature beam, $n(0)$ is the density on axis of other profiles, and N_L is the number of particles per unit length. At high temperatures the space-charge force becomes negligible compared to the external focusing force. Integrating the density over a spatial cross section then leads to $N_L = 4\pi n(0)\epsilon_0 k_B T_\perp \gamma_0^2/q^2 n_0$, which can be substituted into Eq. (4) to get $\lambda_D(0)/a_0 = n_0/2n(0)$. Our values given for $\lambda_D(0)/a_0$ in Table I converge towards this analytic result with increasing temperature.

Lawson listed the ratio $n(0)/n_0$ and $\lambda_D(0)/a_0$ for each of the eight profiles [2]. We could not reproduce his values for $\lambda_D(0)/a_0$, which do not converge towards the limiting value of $n_0/2n(0)$. We attribute this to a possible error in his normalization procedure. Table I shows the numbers for $n(0)/n_0$ and what we believe are the correct values for $\lambda_D(0)/a_0$, with Lawson's results given

TABLE I. List of relevant parameters for the radial Boltzmann density profiles of Fig. 1(a) and the density on axis for Fig. 1(b).

Curve	$n(0)/n_0$	$\lambda_D(0)/a_0$	$\tilde{r}/\tilde{r}_0$	$\overline{\lambda_D}/a$	Ka^2/ϵ^2	k/k_0	$n(0)/n_0(\tilde{r}=\tilde{r}_0)$
1	0.1	4.82(14.6)	4.43	1.52	0.054	0.974	1.96
2	0.25	1.81(3.9)	2.75	0.905	0.153	0.931	1.89
3	0.5	0.795(1.3)	1.88	0.562	0.396	0.846	1.77
4	0.75	0.432(0.58)	1.46	0.374	0.893	0.727	1.60
5	0.95	0.229(0.27)	1.18	0.223	2.51	0.534	1.32
6	0.995	0.145(0.16)	1.08	0.144	6.00	0.378	1.16
7	0.9995	0.107(0.12)	1.04	0.107	10.9	0.290	1.08
7*a*	0.999995	0.071	1.02	0.071	24.8	0.197	1.04
8	1	0	1	0	∞	0	1

in parentheses. In addition, we calculated and listed for each profile the values for the rms radius $\tilde{r}$ divided by the rms ratio $\tilde{r}_0$ of the zero-temperature beam, the ratio of the average Debye length $\overline{\lambda_D}$ to the effective beam radius $a=\sqrt{2}\tilde{r}$, the space-charge parameter Ka^2/ϵ^2, and tune depression k/k_0. The last two parameters are obtained by comparing each profile with the equivalent uniform (K-V) beam having the same rms radius, rms emittance, and generalized perveance $K=(I/I_0)(2/\beta_0^3\gamma_0^3)$, where I is the beam current and $I_0=4\pi\epsilon_0 mc^3/q=mc^2/30q$ the characteristic current. The average Debye length is calculated using the relation $\overline{\lambda_D}/a=[\lambda_D(0)/a_0][n(0)/n_0]^{1/2}$, and the effective emittance ϵ is related to the rms emittance $\tilde{\epsilon}$ by $\epsilon=4\tilde{\epsilon}$. If k and k_0 denote the focusing wave constants with and without space charge, we find the following relation between k/k_0, Ka^2/ϵ^2, and $\overline{\lambda_D}/a$:

$$\frac{\epsilon^2}{Ka^2}=\frac{1}{k_0^2/k^2-1}=8\left(\frac{\overline{\lambda_D}}{a}\right)^2. \tag{5}$$

The last column in Table I shows the density on axis for the case where the profiles are normalized to have the same rms radius (e.g., by increasing the focusing strength).

We next solve the Boltzmann relation for case (B), with a linear external focusing force given by the potential function

$$\phi_{\|e}(z)=\phi_{\|0}\left(\frac{z^2}{z_0^2}-1\right), \tag{6}$$

where $\phi_{\|0}=-\phi_{\|e}(0)$, $\phi_{\|e}=0$ at $z=z_0$, and $z=s-s_0$ is the difference between the position s of a particle and the centroid position s_0. The effective potential function $\phi_{\|s}(z)$ due to the self-fields can be related to the longitudinal line-charge density $\rho_L(z)$ to good approximation by

$$\phi_{\|s}(z)=\frac{g\rho_L(z)}{4\pi\epsilon_0\gamma_0^2}+\text{const}, \tag{7}$$

where g is the geometry factor [6] of order unity that depends on z_m/a, the ratio of the semiaxes z_m and the bunch radius a, and on b/a, the ratio of the conducting tube radius b to the bunch radius. By substituting (6) and (7) into the longitudinal Boltzmann relation one obtains

$$\frac{\rho_L(z)}{\rho_L(0)}=\exp\left\{-\frac{q\phi_{\|0}}{k_BT_\|}\frac{z^2}{z_0^2}+\frac{qg\rho_L(0)}{4\pi\epsilon_0\gamma_0^2k_BT_\|}\left[1-\frac{\rho_L(z)}{\rho_L(0)}\right]\right\}. \tag{8}$$

This can be rearranged to get z as a function of $\rho_L(z)/\rho_L(0)$.

The profiles $\rho_L(z)$ for eight temperatures are given in Fig. 2. In Fig. 2(a) the focusing force is kept constant while the profiles in Fig. 2(b) are normalized to have a constant rms bunch length (for clarity, only four are numbered). For the zero-temperature profile we find that

$$\rho_L(z)=\frac{4\pi\epsilon_0\gamma_0^2q\phi_{\|0}}{qg}\left(1-\frac{z^2}{z_0^2}\right), \tag{9}$$

which represents a parabolic line charge density. In this limit ($T_\|\to 0$), the thermal distribution thus agrees with Neuffer's model [7] in which the line-charge profile is parabolic over all parameter ranges, whereas the thermal profile becomes more Gaussian with increasing temperature, as seen in Fig. 2. The linear behavior of a parabolic line-charge profile in a low-temperature beam with linear external focusing has recently been studied experimentally [8].

Each density profile can be correlated with the equivalent parabolic beam of half length z_m having the same longitudinal rms width $\tilde{z}$ and rms emittance $\tilde{\epsilon}_z=\tilde{z}^2k_z$, where $z_m=\sqrt{5}\tilde{z}$. k_z and k_{z0} are the focusing wave constants with and without space charge and K_L is defined by

$$K_L=\frac{3}{2}\frac{gNr_c}{\beta_0^2\gamma_0^5}=z_m^3(k_{z0}^2-k_z^2), \tag{10}$$

where N is the total number of particles in the bunch and

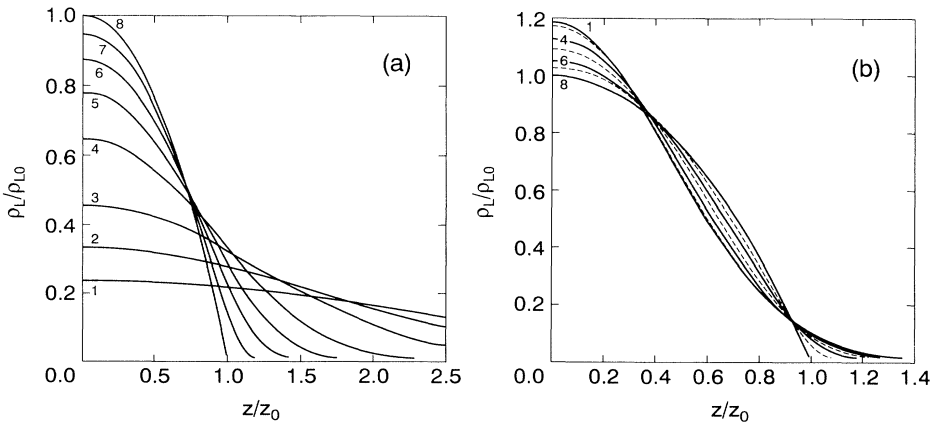

FIG. 2. Line-charge density as a function of longitudinal distance z from the bunch center for different temperatures. (a) Constant focusing and (b) constant rms width. The parameters for each curve are listed in Table II.

TABLE II. Parameter values for the eight longitudinal charge density profiles in Fig. 2(a), and the line-charge density at the center for Fig. 2(b), with an additional profile (7*a*) which is not shown in Fig. 2.

Curve	$k_B T_{\parallel}/q\phi_{\parallel 0}$	$\rho_L(0)/\rho_{L0}$	$\tilde{z}/\tilde{z}_0$	k_z/k_{z0}	$\rho_L(0)/\rho_{L0}(\tilde{z}=\tilde{z}_0)$
1	10	0.237	5.03	0.994	1.19
2	5	0.332	3.59	0.985	1.19
3	2.5	0.455	2.59	0.965	1.18
4	1	0.645	1.76	0.898	1.14
5	0.5	0.777	1.41	0.793	1.10
6	0.25	0.873	1.21	0.653	1.06
7	0.1	0.947	1.09	0.459	1.03
7*a*	0.05	0.974	1.05	0.338	1.02
8	0	1	1	0	1

$r_c = q^2/4\pi\epsilon_0 mc^2$ is the classical particle radius. We find that

$$\frac{k_B T_{\parallel}}{q\phi_{\parallel 0}} = \frac{2}{5}\frac{k_z^2}{k_{z0}^2}\frac{\tilde{z}^2}{\tilde{z}_0^2} \quad \text{or} \quad \frac{k_z}{k_{z0}} = \left(\frac{5}{2}\frac{k_B T_{\parallel}}{q\phi_{\parallel 0}}\right)^{1/2}\frac{z_0}{z_m}, \qquad (11)$$

since $\tilde{z}_0/\tilde{z} = z_0/z_m$.

The results for the tune depression k_z/k_{z0} for the longitudinal particle oscillations shown in Table II have been calculated from Eq. (11). They can be correlated with the longitudinal perveance parameter K_L by Eq. (10).

In conclusion we note that the spatial shape of the thermal distributions for different operating regimes is of fundamental interest and particularly important for the applications mentioned in the beginning. Nonstationary beams, e.g., those with the wrong density profile or mismatched to the focusing channel, relax towards the equilibrium state via emittance growth and halo formation [9–11], and the high-energy Gaussian tails may lead to beam spill across the transverse and longitudinal phase-space boundaries. A more detailed discussion of the beam physics involved and derivation of the relations presented in this Letter will be given in Ref. [1].

This research is supported by the Department of Energy and the Office of Naval Research.

[1] M. Reiser, "Theory and Design of Charged Particle Beams" (Wiley, New York, to be published), Chaps. 5 and 6.

[2] J. D. Lawson, *The Physics of Charged Particle Beams* (Clarendon, Oxford, 1988), 2nd ed., Chap. 4.6.

[3] T. M. O'Neil and C. F. Driscoll, Phys. Fluids **22**, 266 (1979).

[4] I. Hofmann and J. Struckmeier, Part. Accel. **21**, 69 (1987).

[5] See, for instance, D. A. Edwards and M. J. Syphers, *An Introduction to the Physics of High Energy Accelerators* (Wiley, New York, 1993).

[6] See *An Introduction to the Physics of High Energy Accelerators* (Ref. [5]), Chap. 6.2.1, in which the associated longitudinal electric field is given. A more detailed discussion of relation (7) and of the *g* factor is presented in Ref. [1], and in C. Allen, N. Brown, and M. Reiser, "Image effects for bunched beams in axisymmetric systems," Laboratory for Plasma Research, University of Maryland, College Park, Maryland, CPB Technical Report No. 93-045, August 1993 (to be published).

[7] D. Neuffer, IEEE Trans. Nucl. Sci. **26**, 3031 (1979).

[8] D. X. Wang, J. G. Wang, D. Kehne, and M. Reiser, Appl. Phys. Lett. **62**, 3232 (1993).

[9] M. Reiser, J. Appl. Phys. **70**, 1919 (1991).

[10] T. P. Wangler, in *High-Brightness Beams for Advanced Accelerator Applications*, edited by W. W. Destler and S. K. Guharay, AIP Conf. Proc. No. 253 (AIP, New York, 1992), p. 21.

[11] D. Kehne, M. Reiser, and H. Rudd, in *High-Brightness Beams for Advanced Accelerator Applications* (Ref. [10]), p. 47.